

## Phase transitions of hadronic to quark matter at finite $T$ and $\mu_B$

B. Liu<sup>1,2,3</sup>, M. Di Toro<sup>4,5</sup> \*, G.Y. Shao<sup>4</sup>, V. Greco<sup>4,5</sup>, C.W. Shen<sup>6</sup>, and Z.H. Li<sup>7</sup>

<sup>1</sup> *Center of Theoretical Nuclear Physics, National Laboratory of Heavy Ion Accelerator,  
Lanzhou 730000, People's Republic of China*

<sup>2</sup> *Theoretical Physics Center for Scientific Facilities,  
Chinese Academy of Sciences, Beijing 100049, People's Republic of China*

<sup>3</sup> *Institute of High Energy Physics, Chinese Academy of Sciences,  
Beijing 100049, People's Republic of China*

<sup>4</sup> *Laboratori Nazionali del Sud INFN, I-95123 Catania, Italy*

<sup>5</sup> *Physcs and Astronomy Dept., University of Catania, Italy*

<sup>6</sup> *School of Science, Huzhou Teachers College,  
Huzhou 313000, People's Republic of China*

<sup>7</sup> *Institute of modern physics, Fudan University,  
Shanghai 200433, People's Republic of China*

The phase transition of hadronic to quark matter and the boundaries of the mixed hadron-quark coexistence phase are studied within the two Equation of State (EoS) model. The relativistic effective mean field approach with constant and density dependent meson-nucleon couplings is used to describe hadronic matter, and the MIT Bag model is adopted to describe quark matter. The boundaries of the mixed phase for different Bag constants are obtained solving the Gibbs equations.

We notice that the dependence on the Bag parameter of the critical temperatures (at zero chemical potential) can be well reproduced by a fermion ultrarelativistic quark gas model, without contribution from the hadron part. At variance the critical chemical potentials (at zero temperature) are very sensitive to the EoS of the hadron sector. Hence the study of the hadronic EoS is much more relevant for the determination of the transition to the quark-gluon-plasma at finite baryon density and low- $T$ . Moreover in the low temperature and finite chemical potential region no solutions of the Gibbs conditions are existing for small Bag constant values,  $B < (135 \text{ MeV})^4$ .

Isospin effects in asymmetric matter appear relevant in the high chemical potential regions at lower temperatures, of interest for the inner core properties of neutron stars and for heavy ion collisions at intermediate energies.

PACS numbers: 05.70.Ce, 21.65.Mn, 12.38.Mh, 25.75.Nq

---

\* ditoro@lns.infn.it

## 1. Introduction

It has been suggested that a phase transition would take place from hadronic matter to deconfined quark-gluon matter at sufficiently high density and/or high temperature. There has been considerable interest in relativistic heavy-ion collisions which could offer the possibility of producing a hot and dense matter and/or plasma of deconfined quarks and gluons. Up to now, experimental data on the phase transition have been extracted from ultrarelativistic collisions of almost isospin-symmetric nuclei, having a proton fraction  $Z/A \sim 0.4 - 0.5$ , in a region of very small chemical potentials. These experimental data from ultrarelativistic collisions could provide the possibility of studying the phase transition and testing effective QCD models.

The interest in the transition at high baryon and isospin densities has been recently growing from the possibility of using new heavy ion facilities at intermediate energies and for the interest in the properties of the inner core of neutron stars where the transition to deconfined quark matter can likely occur. Now the main problem is that we do not have fully reliable effective QCD theories able to describe the two phases so the main approach has been based on a two-EoS model with the Gibbs conditions. In fact this scheme has been widely used to make predictions on the phase transition in the interior of neutron stars (e.g., see the recent [1, 2] and refs. therein). We remark that, even in the two-EoS approach, only a few papers have studied the phase diagram of hadron-quark transitions at high baryon density in connection to the phenomenology of heavy-ion collision in the ten A GeV range (intermediate energies) [3–7].

In Ref. [3] the phase transition from hadron to quark matter has been firstly analyzed also for isospin asymmetric matter. In this work, a Relativistic Mean Field (RMF) model, involving the interaction of baryons with isoscalar scalar and vector fields and with the isovector  $\rho$  meson and pion field, was used for hadronic matter and a MIT-Bag model involving massless u and d quarks was adopted for quark matter. More recently, Refs.[4, 5], the RMF approach was extended to the isovector-scalar  $\delta$ -field to study symmetry energy effects on the possible formation of a mixed hadron-quark phase at high baryon density during intermediate energy collisions between neutron-rich heavy ions.

We remind that the nonlinear Walecka model (*NLWM*) [8, 9] based on the *RMF* effective theory, has been extensively applied to study the properties of nuclear matter and neutron star, stable nuclei and then extended to the drip-line regions. In the last years some authors [10–14] have stressed the importance of including the  $\delta(a_0(980))$  field in hadronic effective field theories for asymmetric nuclear matter. The role of the  $\delta$  meson in isospin channels appears relevant at high density regions [10–14] and so of great interest in nuclear astrophysics.

In order to describe the medium dependence of nuclear interactions, a density dependent relativistic hadron (*DDRH*) field theory has been also suggested [15–17]. The density dependent meson-nucleon couplings are based on microscopic Dirac-Brueckner (*DB*) calculations [16, 18] and adjusted to reproduce some nuclear matter and finite nuclei properties [15–17]. Recently the density dependent coupling models have been applied to the neutron stars [19].

In this paper, we use the constant coupling (NL-RMF) scheme and the DDRH model for hadronic matter and the MIT bag model for quark matter. We study the phase transition of hadronic to quark matter and in particular the dependence of the boundaries of the mixed hadron-quark coexistence phase on the choice of the Bag pressure. Our study leads to the appearance of a Critical-End-Point of the mixed phase for low values of the Bag parameter. Moreover recently a similar effect due to a

density variation of an effective Bag constant has been observed using a Nambu-Jona Lasinio (NJL) model, with dynamical varying masses for the quark phase [20].

We also want to see the effects of the different hadronic models on boundaries of the mixed phase. We find that the critical temperature at low chemical potential is almost not affected by variation of the hadron EoS and the Bag-constant dependence can be well reproduced by a naive ultrarelativistic massless quark gas model. Conversely the critical chemical potential at vanishing temperature is very sensitive to the EoS of the hadronic part. Furthermore the mixed phase structure at high baryon density is affected by the hadron EoS, especially in isospin asymmetric matter. This has been observed when the isovector-scalar  $\delta$  meson is included and when some density dependence of the isovector meson couplings are introduced.

The present paper is organized as follows. In order to give more emphasis on the new obtained results we report in the Appendices all the details about the effective Equation of State adopted in the two sectors: in Appendix A both models used for hadronic matter are described while in Appendix B we introduce the MIT-Bag model at finite temperature for quark matter.

The Gibbs phase transition conditions are presented in Sect.2. The results are shown and discussed in Sect.3. Sect.4 is devoted to a detailed analysis of the Bag constant dependence of critical end points in temperature and chemical potential. Finally some conclusions are drawn in Sect.5.

## 2. The phase transition

According to the Gibbs conditions for phase transition, the temperatures, the chemical potentials, and pressures of hadronic matter have to be identical to that of quark matter inside the mixed phase. Moreover we must require the conservation of the total baryon and isospin densities :

$$\mu_B^H(T, \rho_B^H, \rho_3^H) = \mu_B^Q(T, \rho_B^Q, \rho_3^Q) , \quad (1)$$

$$\mu_3^H(T, \rho_B^H, \rho_3^H) = \mu_3^Q(T, \rho_B^Q, \rho_3^Q) , \quad (2)$$

$$P^H(T, \rho_B^H, \rho_3^H) = P^Q(T, \rho_B^Q, \rho_3^Q) , \quad (3)$$

$$\rho_B^T = (1 - \chi)\rho_B^H + \chi\rho_B^Q , \quad (4)$$

$$\rho_3^T = (1 - \chi)\rho_3^H + \chi\rho_3^Q , \quad (5)$$

where  $\chi$  is the fraction of quark matter in the mixed phase.

The densities and chemical potentials for hadronic matter are defined as

$$\rho_B^H = \rho_p + \rho_n , \quad \rho_3^H = \rho_p - \rho_n , \quad (6)$$

$$\mu_B^H = \frac{1}{2}(\mu_p + \mu_n) , \quad \mu_3^H = \frac{1}{2}(\mu_p - \mu_n) , \quad (7)$$

and consistently for quark matter we have

$$\rho_B^Q = \frac{1}{3}(\rho_u + \rho_d) , \quad \rho_3^Q = \rho_u - \rho_d , \quad (8)$$

$$\mu_B^Q = \frac{3}{2}(\mu_u + \mu_d) , \quad \mu_3^Q = \frac{1}{2}(\mu_u - \mu_d) , \quad (9)$$

The asymmetry parameters for hadronic and quark matter are defined, respectively,

$$\alpha^H = \frac{\rho_n - \rho_p}{\rho_n + \rho_p}, \quad \alpha^Q = 3 \frac{\rho_d - \rho_u}{\rho_d + \rho_u}, \quad (10)$$

and the total asymmetry is

$$\alpha^T = -\rho_3^T / \rho_B^T. \quad (11)$$

Nucleon and quark chemical potentials, as well as the pressures in the two phases at the fixed asymmetry and a fixed temperature, can be obtained directly from respective EoS, as shown in detail in the Appendices A and B.

In the hadron sector we will use the Non-Linear Relativistic Mean Field models, [10, 12, 21], with different structure of the isovector part, already tested to describe the isospin dependence of collective flows and meson production for heavy ion collisions at intermediate energies, [13, 22, 23]. We will refer to these different Iso-Lagrangians as: i)  $NL$ , where no isovector meson is included and the symmetry term is only given by the kinetic Fermi contribution, ii)  $NL\rho$  when the interaction contribution of an isovector-vector meson is considered and finally iii)  $NL\rho\delta$  where also the contribution of an isovector-scalar meson is accounted for. See details in Appendix A1.

We are well aware that there are several uncertainties on the stiffness of the symmetry energy at high baryon density, mainly due to the lack of suitable data, see the reviews [12, 24]. Therefore we will show also results with effective hadron interactions based on RMF models with density dependent meson-nucleon couplings ( $DDRH$  forces, Appendix A2) that present much softer symmetry terms at high baryon density.

As already mentioned, in the quark phase we use the MIT-Bag Model, Appendix B, where the symmetry term is only given by the Fermi contribution. An important part of this work is the study of the Bag-constant dependence of the transition.

### 3. Results: Properties of the Coexistence Zone

The EOS for hadronic and quark matter is used to calculate the baryon and the quark chemical potentials, as well as the pressures in the two phases at the fixed isospin asymmetry and temperature. We study the phase coexistence region in the  $(T, \rho_B, \rho_3)$  space and even the properties inside the mixed phase [5]. For a fixed value of the total asymmetry  $\alpha^T$  and temperature  $T$ , we find solutions of the *Gibbs* conditions for both cases of  $\chi=0.0$  and  $1.0$ . In this way the boundary of the mixed phase region in the  $(T, \rho_B)$  plane can be obtained. Finally we can get the full phase transition diagram by repeating the procedure.

In our calculations we have used  $m_u = m_d = 5.5 \text{ MeV}$ . We will only consider the two-flavor case ( $q = u, d$ ) in the bag model and the interactions between quarks are neglected as a first step. In fact in this work we are mainly interested in the study of the Bag Pressure dependence of the results. In order to obtain the *binodal* boundaries and the phase diagram, an iterative minimization procedure is adopted in the search for the solutions of the *Gibbs* conditions. In Fig.1 we present the phase diagram of hadronic-quark matter coexistence in  $(T, \rho, \rho_3)$  space with  $B^{1/4}=160 \text{ MeV}$  in the  $NL\rho$  and the  $NL\rho\delta$  models. In order to see the effects of different *RMF* models on the phase diagram, we also use

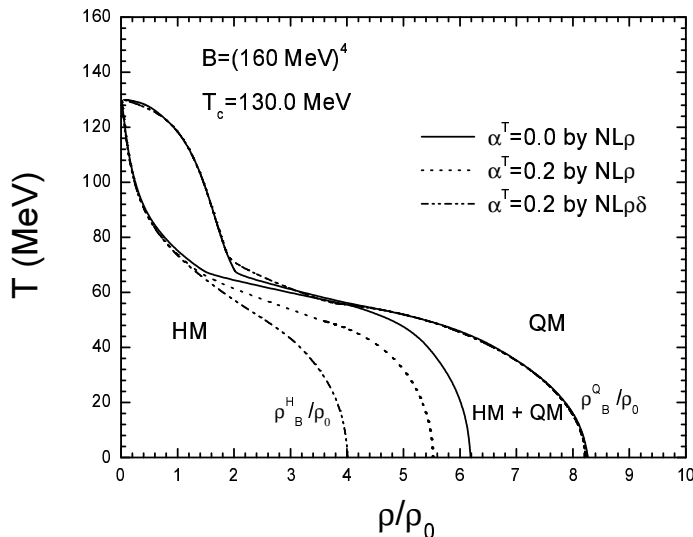


FIG. 1: Phase diagram of hadronic-quark matter coexistence for symmetric matter ( $\alpha^T=0.0$ ) and asymmetric matter ( $\alpha^T=0.2$ ) with  $B^{1/4}=160$  MeV in the  $NL - RMF$  model as a function of the baryon density.

the  $DDRH - RMF$  model to describe the hadronic matter with the same bag constant to calculate the mixed phase coexistence diagram, the results are given in Fig.2.

From Figs.1 and 2 we notice that the main differences between  $NL - RMF$  and  $DDRH - RMF$  models are the boundary densities ( $\rho_B^Q/\rho_0$  and  $\rho_B^H/\rho_0$ ) for the quark and hadronic phases at zero temperature in the isospin asymmetric case. Both models give almost the same critical temperature  $T_c=130$  MeV, which then is not related to hadronic EoS differences as well as to the isospin asymmetry of the matter.

In order to know the effects of different values of the bag constant on the hadronic-quark matter coexistence in  $(T, \rho, \rho_3)$  space, we use  $B^{1/4}=190$  MeV and the two  $RMF$  models to calculate the phase transition diagrams; the results are shown in Figs.3 and 4, respectively. Like in the previous  $B^{1/4}=160$  MeV case, we can see that the behaviors of the binodal boundaries for symmetric matter in the quark and hadronic phases in  $(T, \rho)$  space given by the both  $NL - RMF$  and  $DDRH - RMF$  models are roughly the same.

At variance, for asymmetric matter interesting isospin effects are appearing on the critical points at high baryon density and low temperatures, directly related to the high density behavior of the symmetry energy in the hadron phase [5, 20], see also the discussion in Appendix A. In fact we get that for both Bag-constant choices the boundaries of  $\alpha^T=0.2$  in  $(T, \rho)$  space for the hadronic phase given by  $DDRH\rho$  and  $DDRH\rho\delta$  models are different from that given by  $NL\rho$  and  $NL\rho\delta$  models.

From Figs. 1, 2, 3 and 4, we remark that some squeezing-reopening effects of the binodal surface appear. The squeezing-reopening effect is more evident in the  $B^{1/4}=160$  MeV case and this is due to the variation of the pressure in the quark phase, for a fixed chemical potential  $\mu_B^Q$ , as shown in the following.

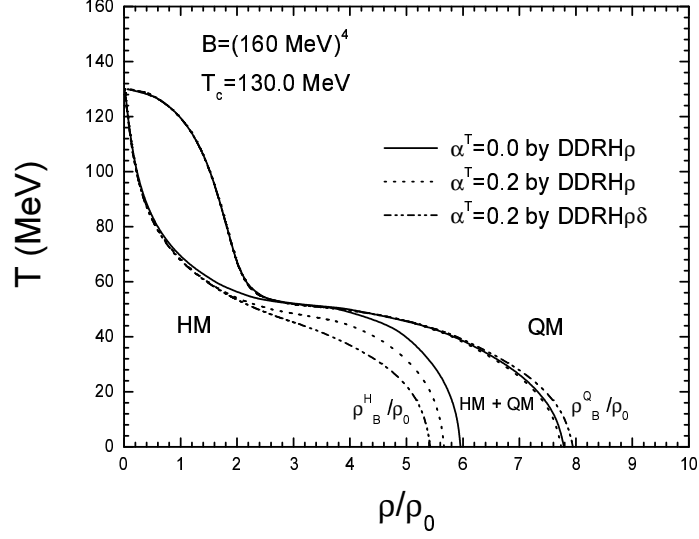


FIG. 2: Same as in Fig.1 in the  $DDRH - RMF$  model.

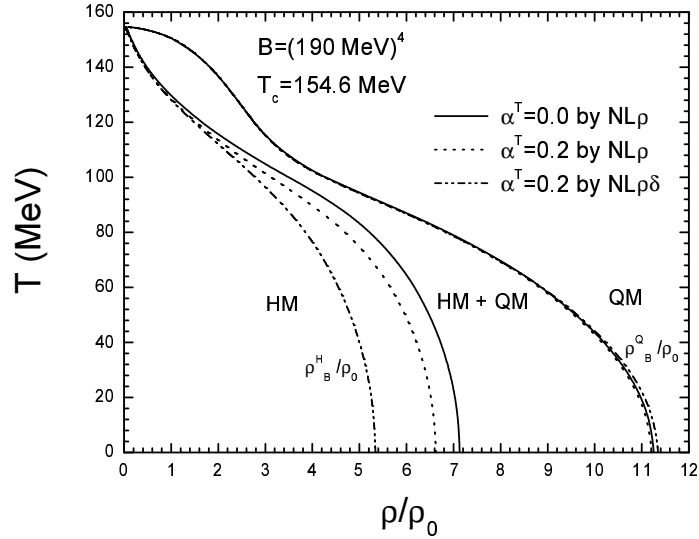


FIG. 3: Same as in Fig.1 with  $B^{1/4}=190 \text{ MeV}$  in the  $NL - RMF$  model.

In order to simplify the discussion we consider the case of symmetric matter,  $\alpha^T=0.0$ , and only the hadronic  $NL$  interaction. First we define the transition chemical potential  $\mu_B^{tr} \equiv \mu_B^H = \mu_B^Q$ . In Fig.5 we plot the transition phase diagrams for symmetric matter in the  $(T, \mu_B)$  space with  $B^{1/4}=160$  and  $190 \text{ MeV}$ , in the  $NL$  model. The inset is the corresponding phase diagram of the transition in the  $(T, \rho)$  space for symmetric matter with  $B^{1/4}=160 \text{ MeV}$ . In order to discuss the squeezing-reopening

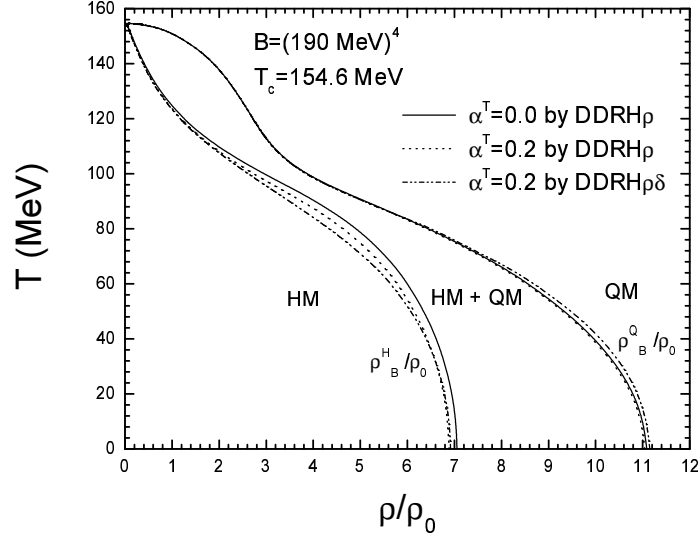


FIG. 4: Same as in Fig.1 with  $B^{1/4}=190$  MeV in the *DDRH* – *RMF* model.

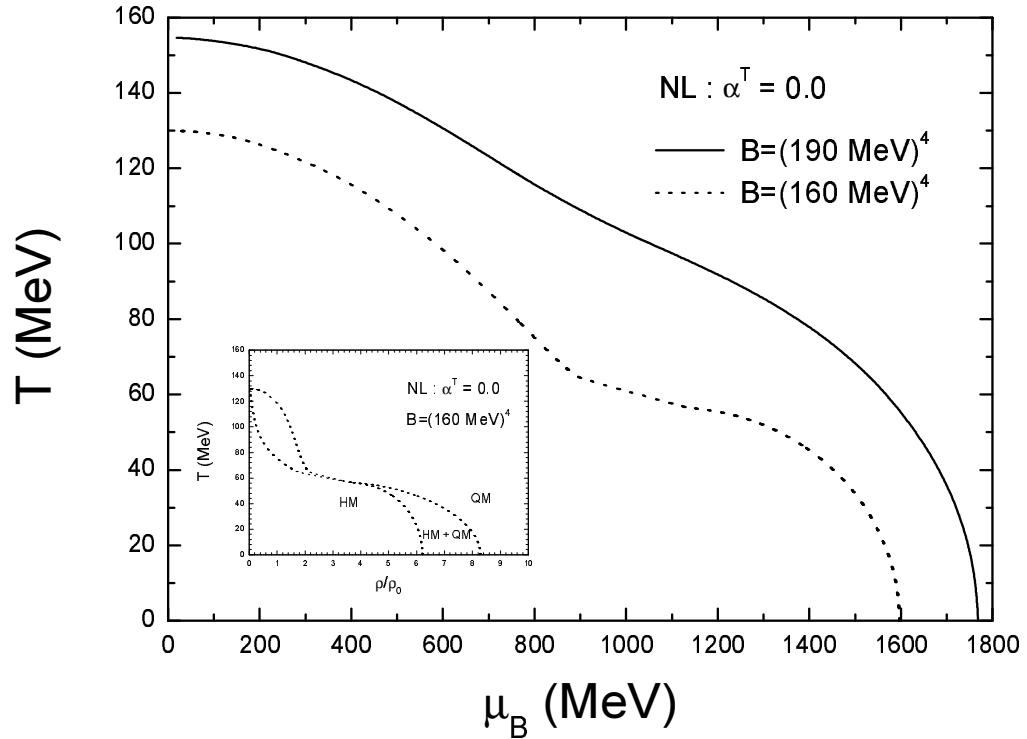


FIG. 5:  $T - \mu_B$  phase diagram in the *NL* $\rho$  model with  $B^{1/4}=160$  and  $190$  MeV. The inset is the  $T - \rho_B$  phase diagram in the *NL* $\rho$  model with  $B^{1/4}=160$  MeV

effect both  $(T, \mu_B)$  and  $(T, \rho)$  phase diagrams should be considered.

If we look at the  $(T, \rho)$  inset in Fig.5, we note that three main regions exist :

(1) The “opening” region at low baryon densities and high temperatures. We can see from Fig.5 that the transition chemical potential  $\mu_B^{tr}$  is smaller than the effective nucleon mass and the effective chemical potentials  $\mu_i^*$  even smaller in this region. This indicates that  $E_i^* > \mu_i^*$  for the hadronic part and the nucleon fermion distribution will be small. So the  $\rho_B^H$  will present a slow increase with  $\mu_B$  ( $f_i(k) \simeq \bar{f}_i(k)$ ). We note that the hadron pressure is mostly of thermal nature and with a positive antifermion contribution in this region. The  $\mu_B$  in the quark part is always much larger than the current quark masses ( $m_u = m_d = 5.5$  MeV) and so we can have a fast increase of the  $\rho_B^Q$ .

(2) The “re-opening” region at high baryon densities and low temperatures. In this region,  $\mu_B$  is larger than the nucleon effective mass. This means that  $E_i^* < \mu_i^*$  for the hadronic part, the nucleon fermion distribution will not be small and so the  $\rho_B^H$  will show a fast increase with  $\mu_B$ , also because the antifermion negative contribution is of course reduced. The interaction part of the hadron pressure shall increase. In correspondence we need a fast increase also of the  $\rho_B^Q$  in order to keep the  $P^H = P^Q$  balance.

(3) The plateau at intermediate region of baryon densities and temperatures. In this region we get  $\mu_B \simeq M^*$  (nucleon effective mass), thus we can have the squeezing of the mixed phase in the  $T - \rho_B$  plane and a kind of plateau in the  $T - \mu_B$  plane. Our study clearly shows that the squeezing-reopening effect on the mixed phase is very sensitive to the value of the MIT bag constant.

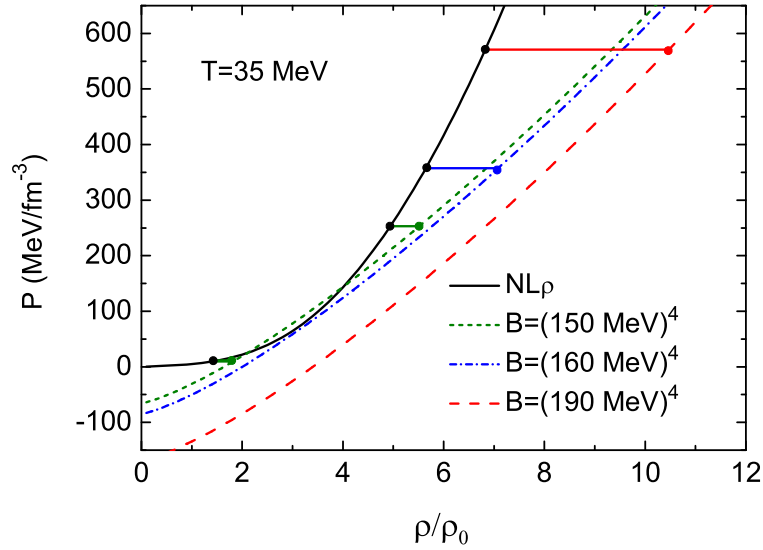


FIG. 6:  $P - \rho_B$  phase diagram of hadronic-quark matter for symmetric matter ( $\alpha_T=0.0$ ) at temperature  $T = 35$  MeV, obtained by the  $NL\rho$  model and various choices of the MIT-Bag constants.

Finally in Fig.6 we present the pressure-baryon density phase diagram of the hadron-quark transition for symmetric matter ( $\alpha_T=0.0$ ) always in the  $NL$  model and for various choices of the MIT-Bag

constant. The temperature is fixed at  $35 \text{ MeV}$ , i.e. in the region of the mixed phase squeezing. The Maxwell constructions are indicated by the connections between the solid line of the hadron pressure and the dashed, dot-dashed and dotted lines of the quark pressure. It can be seen that the squeezing-reopening effect is larger for lower the bag constant choices. In fact for small values of the bag constant we cannot have the solution in the intermediate, flattening, region. This means that the Gibbs conditions cannot be satisfied and we get something like a critical End-Point of the mixed phase. From the figure we see that this is first happening for a Bag constant  $B^{1/4} \simeq 155 \text{ MeV}$ . If we further decrease the Bag pressure we reach the limit of no solutions in general at high chemical potential, since the baryon pressure cannot match the quark pressure, and the mixed phase just disappears. This important result at low temperatures and high densities will be further discussed in detail in the next Section, in particular in connection to the Fig.11.

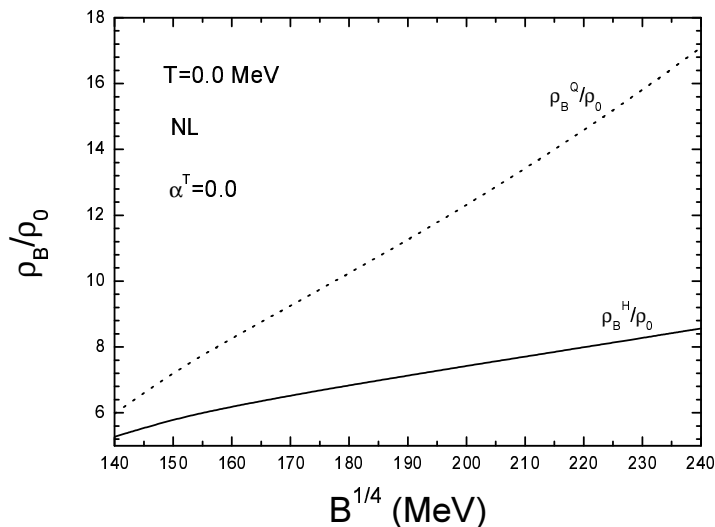


FIG. 7: Baryon and quark densities as a function of the bag constant at  $T=0$ .

#### 4. Dependence of the binodal surface on the Bag constant

We will focus our analysis on results for isospin symmetric matter. In Fig.7 we plot the density boundaries of the binodal region at  $T=0$  as a function of the bag constant  $B^{1/4}$  in the interval 140-240 MeV. The dotted line is the quark matter limit density  $\rho_B^Q/\rho_0$ , the solid line is the hadronic matter limit density  $\rho_B^H/\rho_0$ . We clearly see that both limits are increasing with larger Bag values, as expected from the fact the the energy per particle in the quark phase is increasing. It can be also seen that  $\rho_B^Q/\rho_0$  increases more quickly with the increasing Bag constant than the  $\rho_B^H/\rho_0$ . So the selection of the Bag constant value will influence the binodal surface and in general the final results of the phase transition.

This discussion about Bag constant effects on the transition is more clear in the  $(T, \mu_B)$  plane. Already from Fig.5 (for symmetric matter), where results are reported for  $B^{1/4}= 160$  and  $190 \text{ MeV}$  values, it is evident that the transition region is deeply affected by the choice of the Bag constant,

in particular at the end points at zero temperature or zero chemical potential. We will separately analyze the two regions.

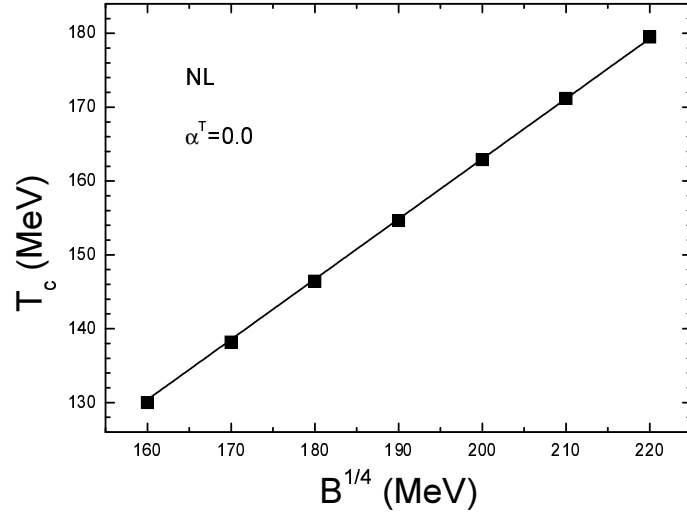


FIG. 8: Critical temperature for symmetric matter ( $\alpha_T=0.0$ ), at zero chemical potential ( $\mu_B = 0$ ), as a function of the bag constant  $B^{1/4}$ . Black Squares: calculated values from Gibbs conditions. Solid line:  $T_c = 0.815B^{1/4}$  fit.

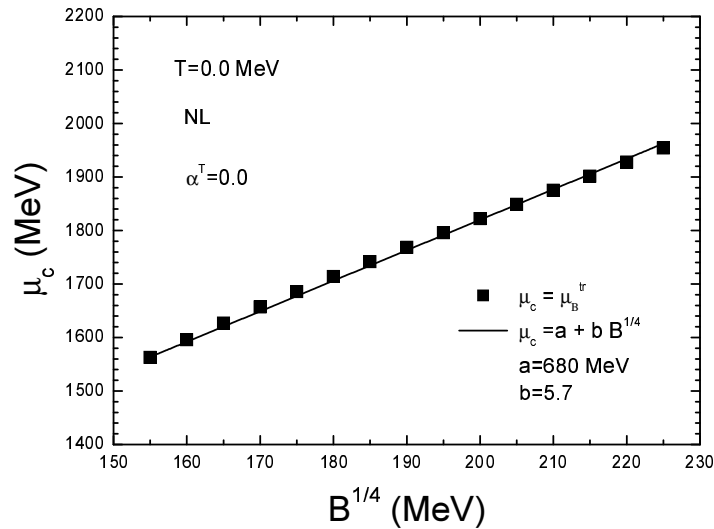


FIG. 9: Critical chemical potential for symmetric matter ( $\alpha_T=0.0$ ), at zero temperature, as a function of the bag constant  $B^{1/4}$ .

In Fig.8 we report the critical temperatures for symmetric matter, at zero chemical potential, for different values of the MIT Bag constant in the 160-220 MeV interval, using the *NL* model for the

hadronic sector. The square points are the calculated values while the solid line is given by the simple linear fit :  $T_c = 0.815B^{1/4}$ .

Similarly in the Fig.9 we show the critical chemical potentials, at zero temperature, for different values of the MIT Bag constant in the same 160-220 MeV interval, always for symmetric matter in the  $NL$  model for the hadronic sector. The square points are the calculated values while the solid line corresponds, even in this case, to a rather simple linear fit :  $\mu_c = a + bB^{1/4}$ , with  $a = 680MeV$  and  $b = 5.7$ . It is interesting to analyze such almost linear behavior of the two end-points as a function of the Bag values, see the following subsection.

Finally, as already noted, we must remark that no  $\mu_c \neq 0$  solutions are existing at zero temperature for very small Bag constants,  $B < (135 MeV)^4$ . This is due to the fact that at low temperature and final chemical potential the hadron pressure, cannot compensate the quark pressure in the coexistence region, as we can also see from Fig.11. Of course this effect is depending on the EoS in the hadron sector. This point will also be discussed in the next subsection.

#### 4.1 Ultrarelativistic gas model

For the quark sector we can use as a reference the naive fermion ultrarelativistic gas model, considering only free quarks in the Bag. Consistently with the results obtained before, no gluons are included. The pressure is simply given by [25, 26]

$$P^Q = \frac{(g_Q + g_{\bar{Q}})}{3} T^4 \left[ \frac{7\pi^2}{120} + \frac{1}{4} \left( \frac{\mu}{T} \right)^2 + \frac{1}{8\pi^2} \left( \frac{\mu}{T} \right)^4 \right] - B \quad (12)$$

where  $g_Q = g_{\bar{Q}} = 12$  is the spin-color-flavor degeneracy factor. The condition  $P^Q = P^H$  will give the critical line of the transition to the quark deconfined matter. Neglecting the hadron contribution ( $P^Q = 0$  condition), from the Eq.(12) we can easily get the two critical end points, at zero chemical potential and at zero temperature, as a function of the Bag parameter.

At  $\mu = 0$  we get a critical temperature

$$T_c = \left[ \frac{30}{7\pi^2} \right]^{1/4} B^{1/4} = 0.81B^{1/4} MeV \quad (13)$$

in a very good agreement with the results obtained from the Gibbs conditions, solid line in Fig.8. The hadron EoS is not contributing to the critical temperature at zero chemical potential, as we can also clearly see from the Figs.1 and 2. The reason is that at  $\mu = 0$  only thermal vacuum excitations contribute to the pressure, ruled essentially by the particle degrees of freedom, which are much larger for the quark phase [26].

This is nicely confirmed by the Fig.10 where we plot the temperature evolution of the pressure in the two phases at  $\mu = 0$ . We see that the hadron pressure is almost negligible up to the crossing points (the  $T_c$  obtained from the full Gibbs conditions). We can estimate an increase at much larger temperatures, due to the onset of anti-hadron contributions, also related to a decrease of the effective nucleon masses..

Of course at  $\mu = 0$  one can argue that the nucleon mass is too high to be thermally excited and in fact it is known that the hadronic matter is now dominated by pions. It is then interesting to compare

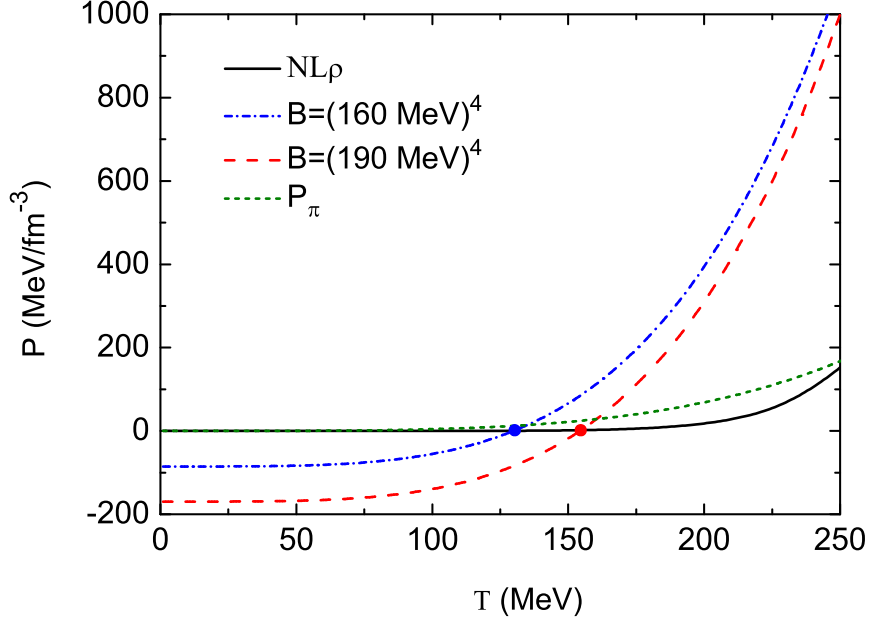


FIG. 10: Symmetric matter ( $\alpha_T=0.0$ ) at zero chemical potential: Hadron pressure (solid, NL choice) and Quark pressure  $P^Q$ , Eq.(12), for various Bag constants (dashed, dot-dashed) as a function of temperature. The dotted line gives the pressure of a massless pion gas, see text. The crossing points correspond to the critical temperatures.

the hadron pressure obtained from the *RMF* approach with the results of a pure massless pion gas pressure  $P_\pi$ , dotted line of Fig.10, given by [26]

$$P_\pi = g_\pi \frac{\pi^2}{90} T^4$$

where  $g_\pi = 3$  is the pion degeneracy. The critical temperatures are almost not affected. A more refined model would be to include all the mesonic resonances with their masses. However this does not significantly change the hadronic pressure up to  $T \simeq 150 - 160 \text{ MeV}$  [27, 28]. We nicely see that the pure thermal hadron pressure is only ruled by the particle degrees of freedom, as already noted.

At variance if we perform the same analysis at  $T = 0$  in order to get the B-dependence of the critical quark chemical potentials we get

$$\mu_c = [2\pi^2]^{1/4} B^{1/4} = 2.11 B^{1/4} \text{ MeV} \quad (14)$$

which corresponds to baryon chemical potential, Eq.(B7),

$$\mu_c^B = \frac{3}{2}(\mu_c^u + \mu_c^d) = 3\mu_c = 6.33 B^{1/4} \text{ MeV} \quad (15)$$

which is in large disagreement with the results obtained from the Gibbs conditions, solid line of Fig.9, corresponding to a linear fit  $\mu_c = a + bB^{1/4}$ , with  $a = 680 \text{ MeV}$  and  $b = 5.7$ , we note two

differences: i) The  $B^{1/4}$  slope is below the 6.33 value expected by the pure quark gas model; ii) We need a constant term  $a = 680 \text{ MeV}$ . Both points are related to density dependence of the hadron interaction, that now cannot be neglected. The different slope comes from interaction contributions to the pressure in the hadron phase. The added constant is due to the presence of the nucleon rest mass in the hadron chemical potential. It is difficult to work out an analytical derivation of these effects since the relation between pressure and chemical potential in the hadron sector is not simple and naive Fermi gas models are largely overestimating the pressures in  $P - \mu_B$  plots [29]. We can only state that at zero temperature and large chemical potentials the critical points are very sensitive to the hadron contribution.

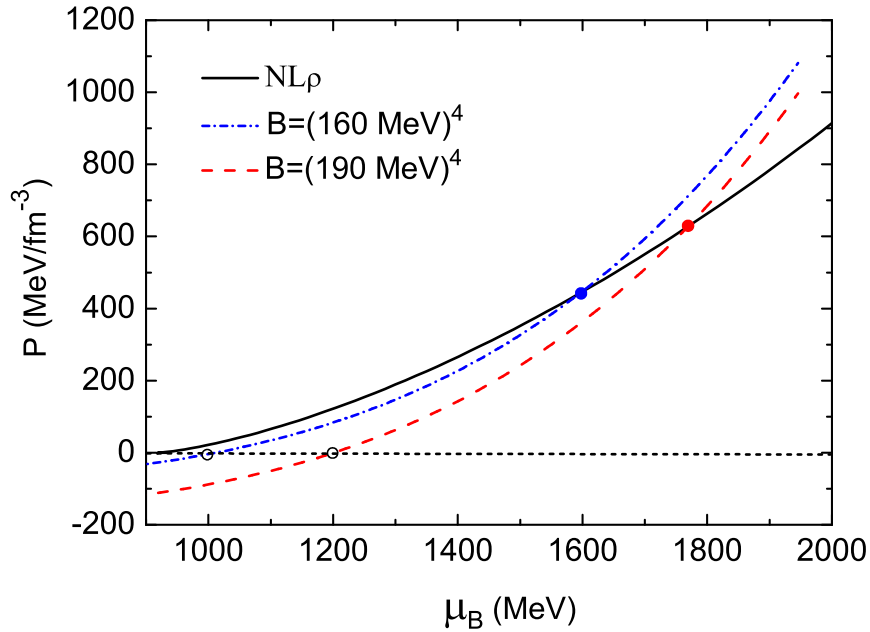


FIG. 11: Symmetric matter ( $\alpha_T=0.0$ ) at zero temperature: Hadron pressure (solid, NL choice) and Quark pressure  $P^Q$  for various Bag constants (dashed, dot-dashed) as a function of baryon chemical potential. We show also  $P^Q = 0$  line corresponding to the case without hadron contribution. The crossing points (solid with the hadron part, open without the hadron contribution) correspond to the critical chemical potentials.

This can be easily seen from Fig.11 where we show the fully calculated pressures  $P^Q$  and  $P^H$  vs. the baryon chemical potential at zero temperature. We show also the points on the line  $P^Q = 0$  corresponding to the deconfinement conditions without hadron contributions. We clearly notice the difference in the crossing points with and without the hadron part. The critical chemical potentials get rather larger values (of about a 50%) with the hadron contribution and also the B-dependence looks different.

Finally we can work out a simple consistency check of the results shown in the Figs. 7 and 9 using the zero temperature relationship between quark chemical potentials and densities  $\rho_q = \mu_q^3/\pi^2$ . Since  $\rho_B^Q = \frac{1}{3}(\rho_d + \rho_u) = \frac{2}{3}\rho_q$  we finally get

$$\mu_B^Q = 3\mu_q = 3\left(\frac{3\pi^2\rho_0}{2}\right)^{1/3}\left(\frac{\rho_B^Q}{\rho_0}\right)^{1/3}(\hbar c) \text{ MeV}$$

Using the critical quark chemical potential parametrization of Fig.9,  $\mu_c = a + bB^{1/4}$ , with  $a = 680 \text{ MeV}$  and  $b = 5.7$ , we nicely get the  $B^{1/4}$  dependence of the quark baryon density limit line of the coexistence region shown in Fig.7.

## 5. Concluding remarks

We use the two kinds of RMF models for hadronic matter, with constant and density dependent couplings, and the MIT-Bag model for the quark matter to study the boundaries of the mixed coexistence phase in the transition from hadronic to quark matter. Binodal surfaces and critical end-points for different isospin asymmetries are obtained using different hadronic models and various MIT Bag constants. The Bag Pressure dependence of the critical points is very interesting since we clearly show the difference between two regions:

- High Temperature and Low Baryon Chemical Potential.

The hadron EoS is not important: we get the same  $T_c$  for any hadron EoS, even including a pure massless pion gas contribution. Isospin effects in asymmetric matter are also negligible. In conclusion the critical temperature at zero chemical potential, when existing, only depends on the value of the Bag constant. In fact we show that if small Bag values are used the binodal surface is shrinking at low densities and finite temperatures and eventually no continuous solutions down to  $\mu = 0$  are found for  $B < (150 \text{ MeV})^4$ .

We note that a  $T_c$  comparison with recent lattice QCD calculations with physical quark masses [28] would indicate an effective Bag constant, at low  $\mu$ , around  $B \simeq (180 - 190 \text{ MeV})^4$ .

- High Baryon Chemical Potential and Low Temperature.

Now we have just the opposite evidence: the Critical Chemical Potential  $\mu_c$  is clearly dependent on the interaction in the hadron phase. Actually we even show that if small Bag values are used the binodal surface is shrinking at high densities and finite temperatures and eventually no  $\mu \neq 0$  solutions are found for  $B < (135 \text{ MeV})^4$ .

Moreover for asymmetric matter all that translates into relevant isospin effects, very sensitive to different symmetry energy terms in the Hadron EoS. These results are of interest for all nuclear systems at high baryon and isospin density and moderate temperature, like neutron star formation and inner core structure and/or heavy ion collisions at intermediate energies.

## Acknowledgments

This work has been partially performed under the FIRB Research Grant RBFR0814TT of the Italian Minister of Education, Universities and Research. This project is supported by the National Natural Science Foundation of China under Grant Nos. 10875160, 11075037, 10979024, 10905021, the Key Project of Science and Technology Research of Ministry of Education of China under grant number 209053, the Natural Science Foundation of Zhejiang Province of China under grant number Y6090210 and the INFN of Italy.

## Appendix A: Equation of state for hadronic matter at finite temperature

### A1. Nonlinear relativistic mean field model with constant couplings

The Lagrangian density, with the isovector scalar  $\delta$  field, used in this work is

$$\begin{aligned} \mathcal{L} = & \bar{\psi}[i\gamma_\mu\partial^\mu - (M - g_\sigma\phi - g_\delta\vec{\tau}\cdot\vec{\delta}) - g_\omega\gamma_\mu\omega^\mu - g_\rho\gamma^\mu\vec{\tau}\cdot\vec{b}_\mu]\psi \\ & + \frac{1}{2}(\partial_\mu\phi\partial^\mu\phi - m_\sigma^2\phi^2) - U(\phi) + \frac{1}{2}m_\omega^2\omega_\mu\omega^\mu + \frac{1}{2}m_\rho^2\vec{b}_\mu\cdot\vec{b}^\mu \\ & + \frac{1}{2}(\partial_\mu\vec{\delta}\cdot\partial^\mu\vec{\delta} - m_\delta^2\vec{\delta}^2) - \frac{1}{4}F_{\mu\nu}F^{\mu\nu} - \frac{1}{4}\vec{G}_{\mu\nu}\vec{G}^{\mu\nu}, \end{aligned} \quad (\text{A1})$$

where  $\phi$  is the  $\phi$ -meson field,  $\omega_\mu$  is the  $\omega$ -meson field,  $\vec{b}_\mu$  is  $\rho$  meson field,  $\vec{\delta}$  is the isovector scalar field of the  $\delta$ -meson.  $F_{\mu\nu} \equiv \partial_\mu\omega_\nu - \partial_\nu\omega_\mu$ ,  $\vec{G}_{\mu\nu} \equiv \partial_\mu\vec{b}_\nu - \partial_\nu\vec{b}_\mu$ , and the  $U(\phi)$  is a nonlinear potential of  $\sigma$  meson :  $U(\phi) = \frac{1}{3}a\phi^3 + \frac{1}{4}b\phi^4$ .

The EOS for nuclear matter with the isovector scalar field at finite temperature in the mean-field approximation (MFA) is given by

$$\begin{aligned} \epsilon = 2 \sum_{i=n,p} \int \frac{d^3k}{(2\pi)^3} E_i^*(k)(f_i(k) + \bar{f}_i(k)) + \frac{1}{2}m_\sigma^2\phi^2 + U(\phi) \\ + \frac{1}{2}\frac{g_\omega^2}{m_\omega^2}\rho^2 + \frac{1}{2}\frac{g_\rho^2}{m_\rho^2}\rho_3^2 + \frac{1}{2}\frac{g_\delta^2}{m_\delta^2}\rho_{s3}^2, \end{aligned} \quad (\text{A2})$$

$$\begin{aligned} P = \frac{2}{3} \sum_{i=n,p} \int \frac{d^3k}{(2\pi)^3} \frac{k^2}{E_i^*(k)}(f_i(k) + \bar{f}_i(k)) - \frac{1}{2}m_\sigma^2\phi^2 - U(\phi) \\ + \frac{1}{2}\frac{g_\omega^2}{m_\omega^2}\rho^2 + \frac{1}{2}\frac{g_\rho^2}{m_\rho^2}\rho_3^2 - \frac{1}{2}\frac{g_\delta^2}{m_\delta^2}\rho_{s3}^2, \end{aligned} \quad (\text{A3})$$

where  $E_i^* = \sqrt{k^2 + M_i^{*2}}$ . The nucleon effective masses are defined as

$$M_i^* = M - g_\sigma\phi \mp g_\delta\delta_3 \quad (- \text{proton}, + \text{neutron}). \quad (\text{A4})$$

The field equations in the relativistic mean field (RMF) approach are

$$\phi = -\frac{a}{m_\sigma^2}\phi^2 - \frac{b}{m_\sigma^2}\phi^3 + \frac{g_\sigma}{m_\sigma^2}(\rho_{sp} + \rho_{sn}), \quad (\text{A5})$$

$$\omega_0 = \frac{g_\omega}{m_\omega^2}\rho, \quad (\text{A6})$$

$$b_0 = \frac{g_\rho}{m_\rho^2}\rho_3, \quad (\text{A7})$$

$$\delta_3 = \frac{g_\delta}{m_\delta^2}(\rho_{sp} - \rho_{sn}), \quad (\text{A8})$$

with the baryon density  $\rho \equiv \rho_B^H = \rho_p + \rho_n$ ,  $\rho_3 \equiv \rho_3^H = \rho_p - \rho_n$  and  $\rho_{s3} = \rho_{sp} - \rho_{sn}$ ,  $\rho_{sp}$  and  $\rho_{sn}$  are the scalar densities for proton and neutron, respectively. The  $f_i(k)$  and  $\bar{f}_i(k)$  in Eqs.(A2)-(A3) are the fermion and antifermion distribution functions for protons and neutrons ( $i = p, n$ ):

$$f_i(k) = \frac{1}{1 + \exp\{[E_i^*(k) - \mu_i^*]/T\}}, \quad (\text{A9})$$

and

$$\bar{f}_i(k) = \frac{1}{1 + \exp\{[E_i^*(k) + \mu_i^*]/T\}}. \quad (\text{A10})$$

where the effective chemical potential  $\mu_i^*$  is determined by the nucleon density  $\rho_i$

$$\rho_i = 2 \int \frac{d^3k}{(2\pi)^3} (f_i(k) - \bar{f}_i(k)), \quad (\text{A11})$$

and the  $\mu_i^*$  is related to the chemical potential  $\mu_i$  in terms of the vector meson mean fields by the equation

$$\mu_i^* = \mu_i - g_\omega \omega_0 \mp g_\rho b_0 \quad (- \textit{proton}, + \textit{neutron}), \quad (\text{A12})$$

where  $\mu_i$  are the thermodynamical chemical potentials  $\mu_i = \partial\epsilon/\partial\rho_i$ . The chemical potentials for proton and neutron are given by, respectively

$$\begin{aligned} \mu_p &= \mu_p^* + \frac{g_\omega^2}{m_\omega^2} \rho + \frac{g_\rho^2}{m_\rho^2} \rho_3 \\ \mu_n &= \mu_n^* + \frac{g_\omega^2}{m_\omega^2} \rho - \frac{g_\rho^2}{m_\rho^2} \rho_3. \end{aligned} \quad (\text{A13})$$

The proton and neutron chemical potentials can be denoted in terms of the baryon and isospin chemical potentials by the equations

$$\mu_p = \mu_B + \mu_3, \quad \mu_n = \mu_B - \mu_3. \quad (\text{A14})$$

The scalar density  $\rho_s$  is given by

$$\rho_s = 2 \sum_{i=n,p} \int \frac{d^3k}{(2\pi)^3} \frac{M_i^*}{E_i^*} (f_i(k) + \bar{f}_i(k)). \quad (\text{A15})$$

### A1.1 Parameters

The isovector coupling constants,  $\rho$ -field and  $\rho + \delta$  cases, are fixed from the symmetry energy at saturation and from Dirac-Brueckner estimations, see the detailed discussions in refs.[10, 30].

The coupling constants,  $f_i \equiv g_i^2/m_i^2$ ,  $i = \sigma, \omega, \rho, \delta$ , and the two parameters of the  $\sigma$  self-interacting terms :  $A \equiv a/g_\sigma^3$  and  $B \equiv b/g_\sigma^4$  are reported in Table 1. The corresponding properties of nuclear matter are listed in Table 2. Here the energy per nucleon is defined  $E/A = \epsilon/\rho - M$ .

**Table 1.** Parameter set.

<i>Parameter Set</i>	NL $\rho$	NL $\rho\delta$
$f_\sigma$ ( $fm^2$ )	10.329	10.329
$f_\omega$ ( $fm^2$ )	5.423	5.423
$f_\rho$ ( $fm^2$ )	0.95	3.150
$f_\delta$ ( $fm^2$ )	0.00	2.500
$A$ ( $fm^{-1}$ )	0.033	0.033
$B$	-0.0048	-0.0048

**Table 2.** Saturation properties of nuclear matter.

$\rho_0$ ( $fm^{-3}$ )	0.16
$E/A$ ( $MeV$ )	-16.0
$K$ ( $MeV$ )	240.0
$E_{sym}$ ( $MeV$ )	31.3
$M^*/M$	0.75

## A2 Density Dependent coupling model

The Lagrangian density, with  $\delta$  meson, now reads

$$\begin{aligned}
\mathcal{L} = & \bar{\psi}[i\gamma_\mu\partial^\mu - (M - g_\sigma\phi - g_\delta\vec{\tau}\cdot\vec{\delta}) - g_\omega\gamma_\mu\omega^\mu - g_\rho\gamma^\mu\vec{\tau}\cdot\vec{b}_\mu]\psi \\
& + \frac{1}{2}(\partial_\mu\phi\partial^\mu\phi - m_\sigma^2\phi^2) + \frac{1}{2}m_\omega^2\omega_\mu\omega^\mu + \frac{1}{2}m_\rho^2\vec{b}_\mu\cdot\vec{b}^\mu \\
& + \frac{1}{2}(\partial_\mu\vec{\delta}\cdot\partial^\mu\vec{\delta} - m_\delta^2\vec{\delta}^2) - \frac{1}{4}F_{\mu\nu}F^{\mu\nu} - \frac{1}{4}\vec{G}_{\mu\nu}\vec{G}^{\mu\nu},
\end{aligned} \tag{A16}$$

where  $\phi$  is the  $\phi$ -meson field,  $\omega_\mu$  the  $\omega$ -meson field,  $\vec{b}_\mu$  the  $\rho$  meson field and  $\vec{\delta}$  the isovector scalar field of the  $\delta$ -meson, respectively.  $F_{\mu\nu} \equiv \partial_\mu\omega_\nu - \partial_\nu\omega_\mu$  and  $\vec{G}_{\mu\nu} \equiv \partial_\mu\vec{b}_\nu - \partial_\nu\vec{b}_\mu$ .

The most important difference to conventional RMF theory is the contribution from the rearrangement self-energies to the DDRH baryon field equation. The meson-nucleon couplings  $g_\sigma$ ,  $g_\omega$ ,  $g_\rho$  and  $g_\delta$  are assumed to be vertex functions of Lorentz-scalar bilinear forms of the nucleon field operators. In most applications of DDRH theory, these couplings are chosen as functions of the vector density  $\hat{\rho}^2 = \hat{j}_\mu\hat{j}^\mu$  with  $\hat{j}_\mu = \bar{\psi}\gamma_\mu\psi$ .

The variational derivative of Lagrangian density Eq. (A16) is

$$\frac{\partial\mathcal{L}}{\partial\bar{\psi}} = \frac{\partial\mathcal{L}}{\partial\psi} + \frac{\partial\mathcal{L}}{\partial\hat{\rho}}\frac{\partial\hat{\rho}}{\partial\bar{\psi}}. \tag{A17}$$

The density dependence of the vertex functions  $g_\sigma$ ,  $g_\omega$ ,  $g_\rho$  and  $g_\delta$  produces the rearrangement contribution  $\Sigma_\mu^R$

$$\Sigma^R = \bar{\psi}\left[\frac{\partial g_\sigma}{\partial\hat{\rho}}\phi + \frac{\partial g_\delta}{\partial\hat{\rho}}\vec{\tau}\cdot\vec{\delta} - \frac{\partial g_\omega}{\partial\hat{\rho}}\gamma_\mu\omega^\mu - \frac{\partial g_\rho}{\partial\hat{\rho}}\gamma^\mu\vec{\tau}\cdot\vec{b}_\mu\right]\psi, \tag{A18}$$

and

$$\Sigma_\mu^R = -\Sigma^R u_\mu, \quad (\text{A19})$$

where  $u^\mu = \frac{\hat{\gamma}^\mu}{\rho}$  is a four-velocity with  $u^\mu u_\mu = 1$ . The Dirac equation takes the conventional form

$$[\gamma_\mu (i\partial^\mu - \Sigma^\mu) - (M - \Sigma^s)]\psi = 0, \quad (\text{A20})$$

where  $\Sigma_\mu = g_\omega \omega_\mu + g_\rho \vec{\tau} \cdot \vec{b}_\mu - \Sigma_\mu^R$  and  $\Sigma_s = g_\sigma \phi + g_\delta \vec{\tau} \cdot \vec{\delta}$ . The field equation of baryon in the mean-field approximation (MFA) is

$$(i\gamma_\mu \partial^\mu - (M - g_\sigma \phi - g_\delta \tau_3 \delta_3) - g_\omega \gamma^0 \omega_0 - g_\rho \gamma^0 \tau_3 b_0 + \gamma^0 \Sigma_0^R)\psi = 0, \quad (\text{A21})$$

with

$$\begin{aligned} \phi &= \frac{g_\sigma}{m_\sigma^2} \rho_s \equiv \frac{g_\sigma}{m_\sigma^2} (\rho_{sp} + \rho_{sn}), \\ \omega_0 &= \frac{g_\omega}{m_\omega^2} \langle \bar{\psi} \gamma^0 \psi \rangle = \frac{g_\omega}{m_\omega^2} \rho \equiv \frac{g_\omega}{m_\omega^2} (\rho_p + \rho_n), \\ b_0 &= \frac{g_\rho}{m_\rho^2} \langle \bar{\psi} \gamma^0 \tau_3 \psi \rangle = \frac{g_\rho}{m_\rho^2} \rho_3 \equiv \frac{g_\rho}{m_\rho^2} (\rho_p - \rho_n), \\ \delta_3 &= \frac{g_\delta}{m_\delta^2} \langle \bar{\psi} \tau_3 \psi \rangle = \frac{g_\delta}{m_\delta^2} \rho_{s3} \equiv \frac{g_\delta}{m_\delta^2} (\rho_{sp} - \rho_{sn}), \\ \Sigma_0^R &= \left( \frac{\partial g_\sigma}{\partial \rho} \right) \frac{g_\sigma}{m_\sigma^2} \rho_s^2 + \left( \frac{\partial g_\delta}{\partial \rho} \right) \frac{g_\delta}{m_\delta^2} \rho_{s3}^2 - \left( \frac{\partial g_\omega}{\partial \rho} \right) \frac{g_\omega}{m_\omega^2} \rho^2 - \left( \frac{\partial g_\rho}{\partial \rho} \right) \frac{g_\rho}{m_\rho^2} \rho_3^2. \end{aligned} \quad (\text{A22})$$

where  $\rho_i$  ( $i = p, n$ ) and  $\rho_{si}$  are baryon and scalar nucleon densities, respectively.

The EoS at finite temperature in the MFA is given by

$$\epsilon = \sum_{i=p,n} 2 \int \frac{d^3k}{(2\pi)^3} E_i^*(k) (f_i(k) + \bar{f}_i(k)) + \frac{1}{2} \frac{g_\sigma^2}{m_\sigma^2} \rho_s^2 + \frac{1}{2} \frac{g_\omega^2}{m_\omega^2} \rho^2 + \frac{1}{2} \frac{g_\rho^2}{m_\rho^2} \rho_3^2 + \frac{1}{2} \frac{g_\delta^2}{m_\delta^2} \rho_{s3}^2, \quad (\text{A23})$$

$$p = \sum_{i=p,n} \frac{2}{3} \int \frac{d^3k}{(2\pi)^3} \frac{k^2}{E_i^*(k)} (f_i(k) + \bar{f}_i(k)) - \frac{1}{2} \frac{g_\sigma^2}{m_\sigma^2} \rho_s^2 + \frac{1}{2} \frac{g_\omega^2}{m_\omega^2} \rho^2 + \frac{1}{2} \frac{g_\rho^2}{m_\rho^2} \rho_3^2 - \frac{1}{2} \frac{g_\delta^2}{m_\delta^2} \rho_{s3}^2 - \Sigma_0^R \rho. \quad (\text{A24})$$

where  $E_i^* = \sqrt{k^2 + M_i^{*2}}$ ,  $i=p,n$ .

The proton and neutron chemical potentials in DDRH model are

$$\begin{aligned} \mu_p &= \mu_p^* + \frac{g_\omega^2}{m_\omega^2} \rho + \frac{g_\rho^2}{m_\rho^2} \rho_3 - \Sigma_0^R \\ \mu_n &= \mu_n^* + \frac{g_\omega^2}{m_\omega^2} \rho - \frac{g_\rho^2}{m_\rho^2} \rho_3 - \Sigma_0^R. \end{aligned} \quad (\text{A25})$$

and the baryon and isospin chemical potentials in the hadron sector consistently defined like before, Eq.(A14).

### A2.1 Parameters of the meson-nucleon coupling density dependence

The parameters of the model include nucleon mass  $M = 939MeV$ , the masses of the mesons  $m_\sigma$ ,  $m_\omega$ ,  $m_\rho$ ,  $m_\delta$  and the density dependent meson-nucleon couplings. The parametrization was proposed [17] as :

$$g_i(\rho) = g_i(\rho_0)f_i(x), \quad for \quad i = \sigma, \omega, \rho, \delta, \quad (A26)$$

with

$$f_i(x) = a_i \frac{1 + b_i(x + d_i)^2}{1 + c_i(x + d_i)^2}, \quad for \quad i = \sigma, \omega, \quad (A27)$$

where  $x = \rho/\rho_0$  and  $\rho_0$  is the saturation density. For  $\rho$  and  $\delta$  mesons, the following parametrization was proposed [31] :

$$f_i(x) = a_i \exp[-b_i(x - 1)] - c_i(x - d_i), \quad for \quad i = \rho, \delta. \quad (A28)$$

The parametrization form and parameters are taken from ref. [17] for  $\sigma$ ,  $\omega$  mesons and ref. [31] for  $\rho$ ,  $\delta$  mesons, respectively. All parameters are listed in Table 3.

**Table 3.** Parameters of the DDRH model.

Model	$TW$ [17]		DDRH $\rho$ [28]	DDRH $\rho\delta$ [28]	
Meson	$\sigma$	$\omega$	$\rho$	$\rho$	$\delta$
$m_i$ (MeV)	550	783	770	770	980
$g_i(\rho_0)$	10.72854	13.29015	3.587	6.476	7.58963
$a_i$	1.365469	1.402488	0.095268	0.095268	0.01984
$b_i$	0.226061	0.172577	2.171	2.171	3.4732
$c_i$	0.409704	0.344293	0.05336	0.05336	-0.0908
$d_i$	0.901995	0.983955	17.8431	17.8431	-9.811

The corresponding density dependence of the couplings is presented in the Fig.12.

### A2.2 Hadronic EoS without and with density dependent couplings

In order to better understand the effects of the density dependence of the nucleon-meson couplings on the hadron-quark phase transition we look here in more detail at the differences on the hadron EoS,  $NL$  vs  $DDRH$  approaches. In Figs. 13, 14, and 15, we show in the order the results for the energy per particle, the pressure and the baryon chemical potential in the case of isospin symmetric case at zero temperature. With density dependent couplings we see a more repulsive hadronic matter and so in general we would expect an “earlier” transition to the quark phase with increasing density.

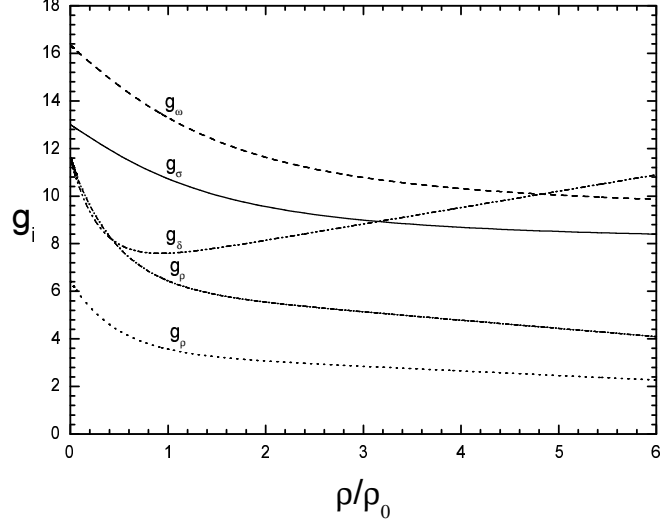


FIG. 12: Density dependence of the meson-nucleon couplings in the used DDRH interactions. The bottom  $g_\rho$  dashed line corresponds to the  $DDRH\rho$  case, without the  $\delta$  meson.

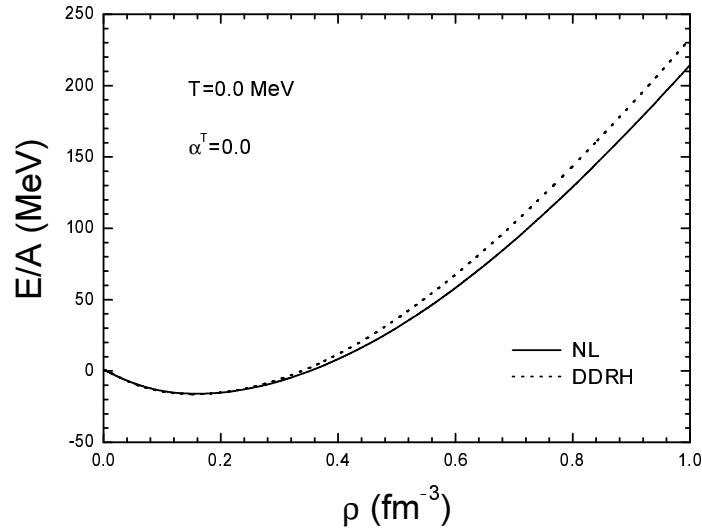


FIG. 13: Energy per nucleon as a function of the baryon density for symmetric matter at  $T=0$ . Solid line: NL results. Dashed line: DDRH.

In any case for symmetric matter the effect will not be too large. In fact we note that the DDRH pressure is not much larger than the NL values. The same is happening for the baryon chemical potentials. This is mostly due to the increase with density of the rearrangement corrections  $\Sigma_0^R \rho$ , Eq.(A24), as shown in the inset of Fig.14.

At variance the effect of density dependent couplings will be noticeably larger in the case of isospin asymmetric matter. In fact at high baryon density the symmetry term will be much reduced due to the decrease of the  $\rho$  – nucleon coupling, see Fig.12. This can be clearly observed from the Fig.16.

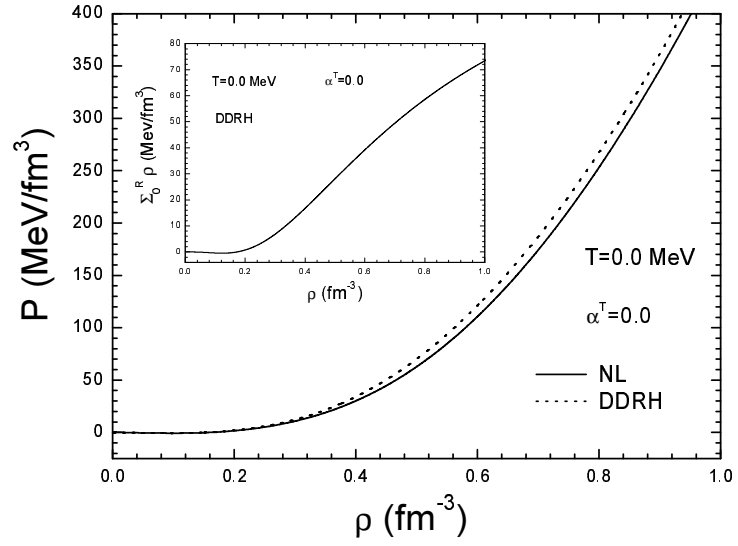


FIG. 14: Pressure as a function of the baryon density for symmetric matter at  $T=0$ . Solid line: NL results. Dashed line: DDRH. In the inset we show the density dependence of the rearrangement term correction to the DDRH pressure

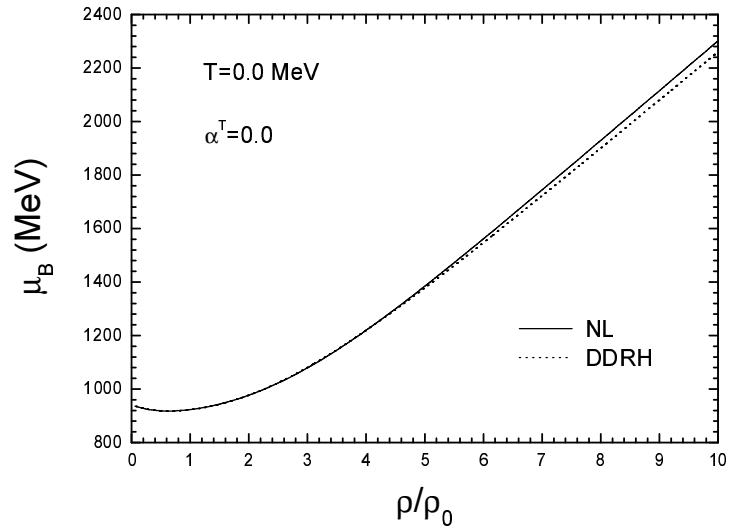


FIG. 15: Baryon chemical potential as a function of the baryon density for symmetric matter at  $T=0$ . Solid line: NL results. Dashed line: DDRH.

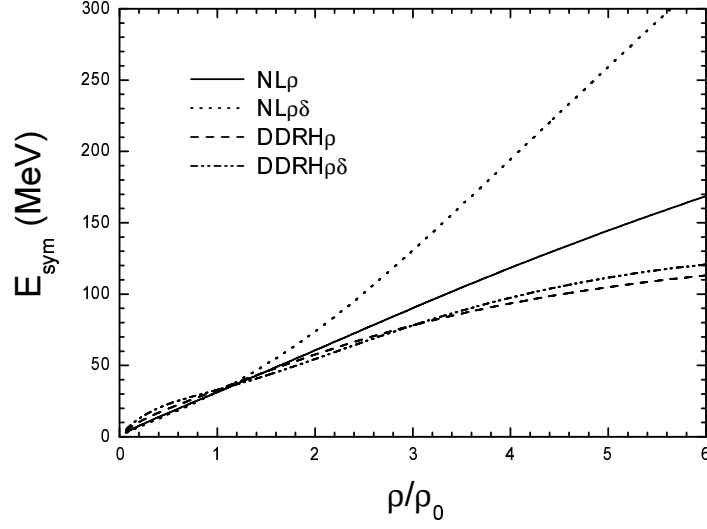


FIG. 16: Symmetry energy as a function of the baryon density at  $T=0$ . Solid and dotted lines:  $NL\rho-\rho\delta$  results with constant couplings. Dashed and dot-dashes lines:  $DDRH$  results with density dependent couplings.

### Appendix B: Quark matter equation of state

The energy density and the pressure for the quark system are, respectively, given by the MIT Bag model [32]

$$\epsilon = 3 \times 2 \sum_{q=u,d,s} \int \frac{d^3k}{(2\pi)^3} \sqrt{k^2 + m_q^2} (f_q + \bar{f}_q) + B, \quad (\text{B1})$$

$$P = \frac{3 \times 2}{3} \sum_{q=u,d,s} \int \frac{d^3k}{(2\pi)^3} \frac{k^2}{\sqrt{k^2 + m_q^2}} (f_q + \bar{f}_q) - B, \quad (\text{B2})$$

where  $B$  denotes the Bag constant (the Bag pressure) chosen as a rather standard parameter [33]. In fact a detailed discussion about the effects of different Bag constants on the hadron-quark transition will be the main topic of this paper.  $m_q$ ,  $q = u, d$ , are the free quark masses (5.5  $MeV$  choice), and  $f_q$ ,  $\bar{f}_q$  represent the Fermi distribution functions for quarks and anti-quarks, respectively :

$$f_q = \frac{1}{1 + \exp\{(E_q - \mu_q)/T\}}, \quad (\text{B3})$$

and

$$\bar{f}_q = \frac{1}{1 + \exp\{(E_q + \mu_q)/T\}}. \quad (\text{B4})$$

where  $E_q = \sqrt{k^2 + m_q^2}$  and  $\mu_q$  are the chemical potentials for quarks and anti-quarks of type  $q$ .

The quark number density is given by

$$n_i = \langle q_i^\dagger q_i \rangle = 3 \times 2 \int \frac{d^3k}{(2\pi)^3} (f_i - \bar{f}_i), \quad i = u, d, \quad (\text{B5})$$

where the chemical potential  $\mu_q$  can be obtained by Eq. (B5) for a given quark number density. The quark number density is  $n_q = n_u + n_d \equiv \rho_q$  and relation with the baryon density is

$$\rho_B^Q = \frac{1}{3} \rho_q = \frac{1}{3} (\rho_u + \rho_d). \quad (\text{B6})$$

The chemical potentials of quarks are related to the baryon and isospin chemical potentials

$$\mu_u = \frac{1}{3} \mu_B + \mu_3, \quad \mu_d = \frac{1}{3} \mu_B - \mu_3. \quad (\text{B7})$$

- 
- [1] G. Y. Shao and Y. X. Liu, Phys. Rev. C **82**, 055801 (2010).  
[2] J. Xu, L. W. Chen, C. M Ko, and B. A. Li, Phys. Rev. C **81**, 055803 (2010).  
[3] H. Müller, Nucl. Phys. A **618**, 349 (1997).  
[4] M.Di Toro, A. Drago, T. Gaitanos, V. Greco, A. Lavagno, Nucl. Phys. A **775**, 102 (2006)  
[5] M.Di Toro, B. Liu, V. Greco, V. Baran, M. Colonna, and S. Plumari, Phys. Rev. C **83**, 014911 (2011).  
[6] G. Pagliara and J. Schaffner-Bielich, Phys. Rev. D **81**, 094024 (2010).  
[7] R. Cavagnoli, C. Providência, and D. P. Menezes, arXiv:1009.3596v1.  
[8] B.D. Serot and J.D. Walecka, Adv. Nucl. Phys. **16**, 1 (1985).  
[9] J. Boguta and A.R. Bodmer, Nucl. Phys. A **292**, 413 (1997).  
[10] B. Liu, V. Greco, V. Baran, M. Colonna, and M. Di Toro, Phys. Rev. C **65**, 045201 (2002).  
[11] D.P.Menezes and C. Providência, Phys. Rev. C **70**, 058801 (2004).  
[12] V. Baran, M. Colonna, V. Greco, M. Di Toro, Phys. Rep. **410**, 335 (2005).  
[13] T. Gaitanos, M. Di Toro, S. Typel, V. Baran, C. Fuchs, V. Greco, H.H. Wolter, Nucl. Phys. A **732**, 24 (2004).  
[14] B. Liu, H. Guo, M. Di Toro, and V. Greco, Eur. Phys. J. A **25**, 293 (2005).  
[15] C.Fuchs, H. Lenske, and H.H. Wolter, Phys. Rev. C **52**, 3043 (1995).  
[16] F. de Jong, H. Lenske, Phys. Rev. C **57**, 3099 (1998); F. Hofmann, C.M. Keil, H. Lenske, Phys. Rev. C **64**, 034314 (2001).  
[17] S.Typel and H.H. Wolter, Nucl. Phys. A **656**, 331 (1999).  
[18] E.N.E. van Dalen, C. Fuchs, Amand Faessler, Nucl. Phys. A **744**, (2004) 227; Phys.Rev. C **72**, (2005) 065803.  
[19] B. Liu, M. Di Toro, V. Greco, C.W. Shen, E.G. Zhao and B.X. Sun, Phys. Rev. C **75**, 048801 (2007).  
[20] G.Y. Shao, M. Di Toro, B. Liu, M. Colonna, V. Greco, Y.X. Liu, *Hadron-quark transition in asymmetric matter with dynamical quark masses*, arXiv:1102.4964v1[nucl-th].

- [21] M. Di Toro et al. *Progr.Part.Nucl.Phys.* **62**, 389-401 (2009).
- [22] V. Greco et al., *Phys.Lett.* **B562**, 215 (2003).
- [23] G. Ferini, T. Gaitanos, M. Colonna, M. Di Toro. H.H. Wolter, *Phys.Rev.Lett.* **97**, 202301 (2006).
- [24] B.A. Li, L.W. Chen, C.M. Ko, *Phys.Rep.* **465**, 113 (2008).
- [25] B. Müller, *The Physics of the Quark-Gluon-Plasma*, Lecture Notes in Physics, Vol. 225, Springer-Verlag, Berlin-Heidelberg 1985.
- [26] K. Yagi, T. Hatsuda, Y. Miaka, *Quark Gluon Plasma*, Ch.3, Cambridge University Press 2005.
- [27] R. Venugopalan, M. Prakash, *Nucl. Phys. A* **546**, 718 (1992).
- [28] S.Boranyi, Z. Fodor, C. Hoelbling, S.D. Katz, S. Krieg, C. Ratti, K.K. Szabo, *JHEP* **09**, 073 (2010); arXiv:1005.3508.
- [29] We remark that the opposite is seen in the  $P - \rho_B$  plane. In fact repulsive vector interaction terms are increasing the pressure for a fixed density but meanwhile also the chemical potential is increasing, see the Appendix A.
- [30] V. Greco, M. Colonna, M.Di Toro, F. Matera, *Phys. Rev. C* **67**, 015203 (2003).
- [31] S.S Avancini, L. Brito, D.P. Menezes, and C. Providencia, *Phys. Rev. C* **70**, 015203 (2004).
- [32] A. Chodos, et al., *Phys, Rev. D* **9**, 3471 (1974).
- [33] K. Schertler, C. Greiner, P.K. Sahu, M.H. Thoma, *Nucl. Phys. A* **637**, 451 (1998).